

# Bullet Clusters in the MareNostrum Universe

Jaime E. Forero-Romero<sup>1</sup>, Stefan Gottlöber<sup>1</sup> and Gustavo Yepes<sup>2</sup>

<sup>1</sup> *Astrophysikalisches Institut Potsdam, An der Sternwarte 16, 14482 Potsdam, Germany ;  
jforeo@aip.de*

<sup>2</sup> *Grupo de Astrofísica, Universidad Autónoma de Madrid, Madrid E-28049, Spain*

## ABSTRACT

We estimate the expected distribution of displacements between the dark matter and gas cores in simulated clusters. We use the MareNostrum Universe, one of the largest non radiative, SPH  $\Lambda$ CDM cosmological simulations. We find that projected 2-D displacements between dark matter and gas, equal or larger than the observed in the Bullet Cluster, are expected in 1% to 2% of the clusters with masses larger than  $10^{14} h^{-1} M_{\odot}$ . The 2-D displacement distribution is roughly the same between redshifts  $0 < z < 0.5$  when multiplied by a factor of  $(1+z)^{-1/2}$ . We conclude that the separations between dark matter and gas as observed in the bullet cluster can be easily found in a  $\Lambda$ CDM universe. Furthermore we find that the displacement distribution is not very sensitive to the normalization of the power spectrum. Upcoming surveys could extend the measurements of these displacements between dark matter and gas into large samples of hundreds of clusters, providing a potential test for  $\Lambda$ CDM.

## 1. Introduction

The standard model of structure formation describes the Universe as a three-component fluid (dark matter (DM), gas and radiation) plus a cosmological constant. There is a fundamental intrinsic difference between the two matter components: while the DM can be modelled in a very good approximation as collisionless fluid, the gaseous component has an evolution dominated by collisional physics. As the interaction between DM and baryons is only through gravitational forces, one can expect a decoupling between the components when the collisional nature of baryons becomes important.

From the observational point of view, the decoupling is evident in collisions of high mass clusters, observed, for the first time, in the cluster 1E0657-56 (Clowe et al. 2006), dubbed the Bullet Cluster. For this object, a combined analysis of strong and weak gravitational lensing and X ray observations gives a displacement of around 200 kpc between the density

peak of the gaseous and dark matter components in the cluster. More examples are given in Dupke et al. (2007); Mahdavi et al. (2007); Jee et al. (2007); Bradač et al. (2008); Jee et al. (2005a,b) but also see Heymans et al. (2008) and the peculiar case in Qin et al. (2008). The standard explanation for this decoupling between DM and gas, is the collision between clusters of galaxies. For example, in the case of a collision between two clusters of comparable mass, the DM halos and galaxies go through each other without falling apart from two body trajectories while the intra-cluster medium, dominated by pressure effects, is stripped out of the DM halos.

In the Bullet Cluster, the expected configuration is that of a massive sub-structure passing close to the center of the cluster, stripping away the gas from the center of both structures, leaving two almost gas-naked cores of dark matter and one single gas core in the middle. The velocity of the expected collision could be inferred observationally from the temperature of the bow shock that is usually present in the collisions (Dopita & Sutherland 2003). N-body simulations (e.g. Springel & Farrar (2007), Mastropietro & Burkert (2008)) support the model but show also that the velocity estimation should be taken with care since the velocity of the encounter between dark matter structures has large statistical and systematic uncertainties when it is derived from the available observations.

The Bullet Cluster has been recognized as potential stringent test for models of structure formation. On one hand it vindicated strongly the need for a dark matter component, but on the other hand it raised doubts on the likelihood of having such extreme events in a  $\Lambda$ CDM universe (Nusser 2008). Hayashi & White (2006) attempted to calculate the probability of finding large velocity collisions such as the one guessed for the Bullet Cluster. They used a large pure DM N-body simulation (the Millennium Run, Springel et al. (2005)) and had to rely then on the information of the possible collisional velocities of substructures inside a cluster sized DM halos. Taking into account the difficulties in the interpretation of the data, the observed velocities can be explained within the framework of  $\Lambda$ CDM. Nevertheless, the frequency of such events changes from 1 to 5 in every 500 clusters, depending on the assumptions made on the velocities of substructures. The lowest value corresponds to the probability of having the sub-structure moving out of the center of the cluster.

The downside of Hayashi & White (2006) is that:

1. The mass assumed for the Bullet Cluster is lower than the most recent estimates. Using the updated mass and the same velocity constraints, the Bullet probability falls to  $10^{-7}$  (Farrar & Rosen 2007)
2. Their results had to be extrapolated from the data in the Millennium simulation, given that the abundance of clusters of comparable mass is not high enough to perform a

more straightforward statistical study.

Both problems have been recently addressed by Lee & Komatsu (2010). They use the MICE dark matter only simulation with  $\sim 200$  times larger volume than the Millennium Run. They use the same approach of finding large relative velocity of DM configurations. The large volume in the MICE simulation allows them to gather a sample of clusters with masses similar to the Bullet Cluster mass. Using the more stringent conditions on the collision velocity, they find that the probability of finding a system similar to the Bullet Cluster is between  $3.3 \times 10^{-11}$  and  $3.6 \times 10^{-9}$ .

Yet, there is another indisputable and clear example of a Bullet-like configuration. The observations of the cluster MACS J0025.4-1222 (Bradač et al. 2008) confirm the existence of two gas naked matter cores and one single hot gas core. As opposed to the case of the original Bullet Cluster, one cannot observe the X-ray emission from the bow-shock. The derivation of a characteristic collision velocity, from a simulation and available observations, can thus lead to confusing and equivocal results. In these two cases the only common and solid observational physical characteristic that can be measured is the separation between the dominant gas clump and the principal dark matter clump.

It is expected that not all the cases of Bullet like configurations, will show a bow-shock X-ray emission, which can constrain the sub-structure velocity (Shan et al. 2010). Therefore, the results of the analysis of dark matter only simulations cannot properly address the likelihood of events similar to the cluster MACS J0025.4-1222. If one wants to use the only robust and accessible observational feature, namely the distance between the dominant DM and gas clumps, to test the  $\Lambda$ CDM model predictions, then one has to resort to hydrodynamical simulations which include a description of the gas in clusters.

Furthermore, as the number of observed clusters increases and will increase even faster with upcoming surveys like eRosita, LSST and Pan-STARRS, we are approaching an era in which a statistical study of this decoupling would become possible through weak lensing and galaxy number counts as a proxy for DM distribution and the X-ray emission as a tracer of the gas component. As a first step in this direction Shan et al. (2010), studied a compilation of 38 clusters. They found 13 objects in which the separation between the center of mass of the gas clump and of the dark matter halo is greater than 50 kpc and 3 more clusters in which the separation is greater than 200 kpc.

The purpose of this paper is to aboard the likelihood of this decoupling from the point of view of the distance between the DM and gas cores in clusters measured in one of the largest volume hydrodynamical simulations done up to now: the so-called *MareNostrum Universe* (Gottlöber & Yepes 2007).

The structure of the paper is as follows: In Section 2 we present the main features of the simulations, in Section 3 we define the algorithm to find the separation between gas and DM structures. In Section 4 we present the probability of finding a cluster with a given projected displacement on the sky. We inspect in Section 5 the dependence of that probability with respect to the normalization of the initial power spectrum. In Section 6 we scrutinize whether the Bullet Cluster should be considered as a challenge to  $\Lambda$  CDM in the context of our study. We summarize our results and state our conclusions in Section 7.

## 2. Simulation

The analysis presented in this paper uses mainly the MareNostrum Universe SPH cosmological simulation described in Gottlöber & Yepes (2007). This non-radiative simulation was run using the GADGET2 TreePM+SPH code Springel (2005) and follows the evolution of gas and dark matter from  $z=40$  to  $z=0$  in a comoving cube of  $500 h^{-1}\text{Mpc}$  on a side. The cosmology used corresponds to the spatially flat concordance model with the following parameters: the total mass density  $\Omega_m = 0.3$ , the baryon density  $\Omega_b = 0.045$ , the cosmological constant  $\Omega_\Lambda = 0.7$ , the Hubble parameter  $h = 0.7$ , the slope of the initial power spectrum  $n = 1$  and the normalization  $\sigma_8 = 0.9$ . The number of particles used for each of the DM and gas component was  $1024^3$ , resulting in a mass of  $8.3 \times 10^9 h^{-1} M_\odot$  for the DM particles and  $1.5 \times 10^9 h^{-1} M_\odot$  for the gas particles. The spatial force resolution was set to an equivalent Plummer gravitational softening of  $15 h^{-1}\text{kpc}$  comoving.

In order to study resolution effects on the distance determination, we have also used a lower resolution simulation run from the same initial conditions as the MareNostrum Universe. Here, the number of particles is  $2 \times 512^3$  and the gravitational smoothing length is correspondingly  $\epsilon \sim 25 h^{-1}\text{kpc}$ . We have performed two more simulations with the same number of particles but different cosmological parameters (equivalent to those obtained from fitting the 3rd year of WMAP data (Spergel et al. 2007)) and two different power spectrum normalizations, a low  $\sigma_8 = 0.75$  and a medium  $\sigma_8 = 0.8$ . The objective is to quantify the effect of that cosmological parameter on the separation probabilities. In Table 1 we summarize the main features of our simulations. More details of these simulations can be found elsewhere (Yepes et al. 2007).

We analyse in the following a non-radiative simulation of a large cosmological volume. It is well known that this approximation fails if one considers the inner regions of clusters (within about 0.1 of the virial radius). However, the outer regions of clusters are nearly self-similar and different simulations agree in a remarkably successful description of the temperature profile in the outside regions of clusters. There are many studies of the formation

of isolated clusters which take into account cooling processes and star formation, however these simulations still fail to describe the inner structure of clusters correctly. Most probably additional processes, like AGN feedbacks, should be taken into account for a proper description. In a recent review, Borgani and Kravtsov (Borgani & Kravtsov 2009) discuss in great detail the issue of cosmological simulations of galaxy clusters. In any case, the statistical study of cluster mergers needs a large simulation volume and large number of particles to properly resolve the merger physics. This task is not yet possible to be done when radiative physics is also considered. Furthermore, there are studies that suggest that the incomplete and rough non-radiative description provides a fair approximation to the dynamics of the gas peaks (Poole et al. 2006).

### 3. Separation Measurement Algorithm

The aim of our analysis is to obtain the distribution of displacements between the dominant density peaks of the DM and gas components of each selected cluster in the simulation. We describe first the algorithm used on a set of hierarchical friend-of-friends (FOF) catalogs. Then, we describe briefly a different and more complex algorithm of structure detection, which, nevertheless, gives the same statistical results than the hierarchical FOF.

#### 3.1. FOF Based Algorithm

We have analysed all simulations with the hierarchical friend-of-friends (FOF) algorithm (Klypin et al. 1999) used for the DM and gas particles, separately. The basic FOF groups were identified using a linking length of  $b = 0.17$  times the mean inter particle separation both for the gas and the DM distribution. The substructures inside the FOF groups are defined as FOF objects constructed with shorter linking lengths  $b_n = b/2^n$  ( $n=1,2,3$ ). We name these catalogs  $\text{FOF}_n^{DM}$  and  $\text{FOF}_n^{gas}$  with ( $n=0,1,2,3$ ) for the DM and gas components

Name	Particles	$\sigma_8$	$\Omega_M$	$\Omega_\Lambda$	$n$
MN-1024	$2 \times 1024^3$	0.9	0.30	0.70	1
MN-512	$2 \times 512^3$	0.9	0.30	0.70	1
MN-512-MS	$2 \times 512^3$	0.8	0.24	0.73	0.95
MN-512-LS	$2 \times 512^3$	0.75	0.24	0.73	0.95

Table 1: Summary of the main characteristics of the four simulations used in this work.

Redshift	# Selected Clusters	Most massive cluster
$z$		$(10^{14} h^{-1} M_{\odot})$
0	4063	25
0.3	2662	20
0.5	1826	13

Table 2: Analyzed redshifts  $z$ , number of selected clusters with  $M > 10^{14} h^{-1} M_{\odot}$  and mass of the most massive cluster at the given redshift in the simulation volume

Mass bin	Minimum Mass	Maximum Mass	# Halos	# Halos	# Halos
	$M_h [10^{14} h^{-1} M_{\odot}]$	$M_h [10^{14} h^{-1} M_{\odot}]$	$z = 0$	$z = 0.3$	$z = 0.5$
1	1.00	1.12	616	463	352
2	2.00	25.0	1403	759	409

Table 3: Mass bins ranges for the different redshift analysis. The last three columns show the number of halos in that bin at a given redshift.

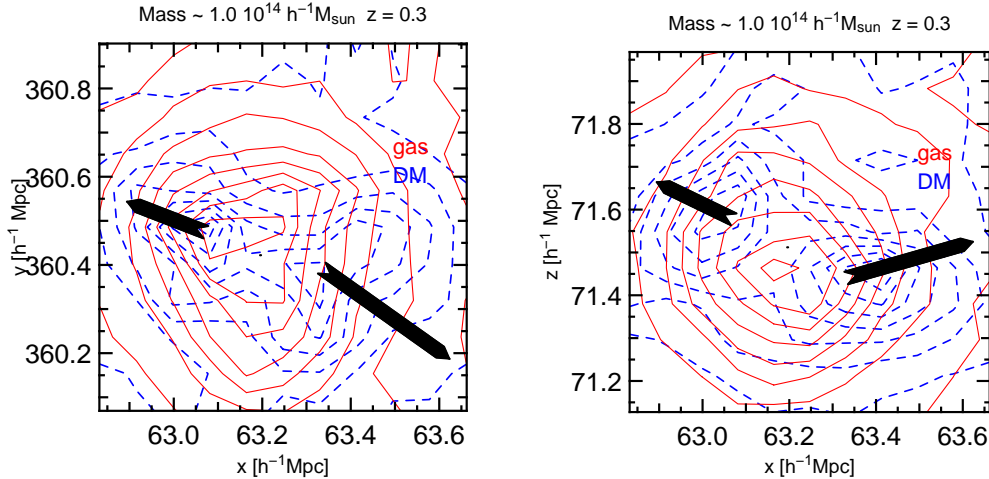


Fig. 1.— Linearly spaced surface density contours for the DM (dashed blue) and gas (continuous red) components of one of the halos with a high displacement seen in two different projections. The arrows are proportional to the velocities respect to the center of the gas core. The cluster of mass  $1.0 \times 10^{14} h^{-1} M_{\odot}$  is located at redshift  $z = 0.3$ , the coordinates are comoving and the relative speed between the two dark matter cores is 560 km/s. In this case, the physical displacement between the centers of gas and DM is of the order of the observed cluster MACS J0025.4-1222.

respectively. For more details on the simulation, the FOF identification and general cluster properties we refer the reader to Gottlöber & Yepes (2007).

For our analysis we have selected all halos with masses larger than  $10^{14}h^{-1}M_{\odot}$ , at four different redshifts,  $z=0, 0.3$  and  $0.5$ . The number of selected halos for every redshift, and the highest halo mass are quoted in Table 2.

Our objective is to measure the physical separation between the dominant gas clump in the cluster, with respect to its predominant DM structure. We find the separation based on the FOF catalogs described above. The main advantage of the FOF algorithm is that it can be easily applied to the subsets of DM particles and gas particles and identifies gas clumps even if they don't have a pronounced density peak. Moreover, the set of linking lengths in the hierarchical FOF allows to find objects at different overdensities. In order to test the robustness of the results from the algorithm based on FOF catalogs we have compared them with those obtained using a spherical overdensity algorithm, the Amiga Halo Finder, described in the next section.

We define the clusters as the objects detected in the DM FOF<sub>0</sub> catalog. FOF<sub>0</sub> provides objects with about virial overdensity, whereas FOF<sub>*i*</sub> provides substructures with about  $8^i$  higher densities. In the MN-1024 simulation a typical object of  $10^{14}h^{-1}M_{\odot}$  at the low mass end of our sample consists of  $\sim 10000$  DM particles and about the same number of gas particles. In the series of low resolution simulations we consider only clusters with masses larger than  $3.2 \times 10^{14}h^{-1}M_{\odot}$  which consists of  $\sim 4000$  DM particles and about the same number of gas particles.

In all cases we find that the clusters exhibit a massive dominant gas clump and various DM clumps. In both DM and gas catalogs we define the dominant clump position in the following way. We identify first the center and radius of the cluster as given by the DM FOF<sub>0</sub> catalog. Next we find the most massive group in the FOF<sub>1</sub> catalog with its center inside the radius defined previously. The clump defines a new center and radius. We iterate this procedure until we cannot find a new group in the following FOF<sub>*i*</sub> catalog. The outputs of the algorithm are the mass and radius of the cluster defined from the DM FOF<sub>0</sub> catalog and the centers of mass of the dominant DM and gas clumps as well as their separation.

It is well known that the FOF algorithm at the level FOF<sub>0</sub> will connect two clusters that are starting to merge as one FOF object. Since such cases could lead to spurious large separations between the DM and gas centers they have been excluded from the analysis. These cases represent always less than 3% of the total number of clusters.



### 3.2. AHF Based Algorithm

As an example of a spherical overdensity halo finder we have used the Amiga Halo Finder (AHF)<sup>1</sup> which identifies both halos and subhaloes. AHF locates local overdensities in a adaptively smoothed grid as prospective halo centers. AHF is described in detail in Knollmann & Knebe (2009).

The AHF algorithm proceeds by creating a hierarchy of grids. High refined grids are spanned in high density regions until a minimum number of particles per grid-cell is reached. The algorithm includes a criterion to span a new mesh refinement, which is usually expressed as a density threshold. To find the positions of the gas and DM clumps we run AHF over the gas and dark matter distribution separately. Thus the positions can be associated to the regions where the corresponding mesh refinement reached its highest level.

In the studied range of separations the two algorithms give the same answers within the simulation uncertainties. We are confident that our results are robust for the range of observed Bullet Cluster displacements. We proceed the rest of the analysis in this paper using the hierarchical FOF algorithm, which is less computationally expensive and much faster than the AHF one.

## 4. Cumulative Probability Distributions

We found simulated clusters that show larger separations than the observed Bullet Cluster or the cluster MACS J0025.4-1222. We checked by visual inspection all the cases where the separation between DM and gas peaks is larger than 200 kpc. All of them correspond to perturbed clusters. In Figure 1 we show one example. The cluster was selected because of its striking similarity to the observed configuration in MACS J0025.4-1222.

We have also checked the dynamical state of two different samples of the clusters at redshift zero. The first sample included those with large displacements ( $> 200$  kpc) and the second sample comprises all clusters with low displacement ( $< 10$  kpc) between gas and dark matter. We found that, indeed all clusters with large displacements come from plunging substructures. Moreover, those clusters which show the most extreme displacements also present a rich variety of merging configurations, with triple DM cores in some cases. On the other hand, in all the cases of clusters with low displacements, the dominant gas blob has a

---

<sup>1</sup>It is a MPI+OpenMP hybrid halo finder to be downloaded freely from <http://www.popia.ft.uam.es/AMIGA>



unique dark matter core associated to it, with practically zero relative velocity between them. A detailed analysis and classification of all configurations giving rise to large displacements in the simulated cluster will be presented in a forthcoming paper.

From the simulations, we know the three dimensional positions of the dominant DM and gas clumps. In order to compare our results with observations, we use 2D projections of the 3D displacements into 10 different randomly selected directions. We quantify the results using the cumulative distribution of the projected 2D displacements. Using the 10 different 2D displacement distributions we bin logarithmically the data in distance and find the mean value and dispersion for the corresponding cumulative distribution.

In the following subsections we study the scaling with mass and redshift of the calculated 2-D displacement cumulative distributions.

#### 4.1. Scaling with Cluster Mass

In Figure 2 we present the cumulative distribution of projected 2D displacements in the MN-1024 simulation. We bin the selected clusters in mass, and calculate the distribution for the 2D physical displacements. The two different mass bins are described in Table (3). The mass bins are selected in such a way as to have a similar number of clusters in each bin at  $z = 0.5$ . We find that, at  $z = 0$ , the fraction of clusters with small physical separations ( $\leq 200\text{kpc}$ ) increases with cluster mass. In contrast, at redshifts  $z = 0.3$  and  $z = 0.5$  we cannot assert that this trend with halo mass exists at all. In any case, in the range of the Bullets displacements, the distributions of different mass bins are less than 1% apart for all the redshifts considered here. As can be seen in the figure, the fraction of simulated clusters with a displacement equal or larger than the observed ones is always between 1% and 2%. The lowest value corresponds to the less massive clusters at  $z = 0$  and the highest value is associated with clusters at high redshifts  $z \sim 0.5$ .

The statistical properties of the displacements at redshift  $z = 0.3$ , for masses larger to  $1.0 \times 10^{15} h^{-1} \text{M}_{\odot}$ , is nevertheless very poor. We find a small sample of 8 clusters. An insufficient number to make a solid statistical statement. In spite of that, we found 1 cluster, from the sample of 8 clusters, with a 3D displacement larger than the one measured in the Bullet Cluster.

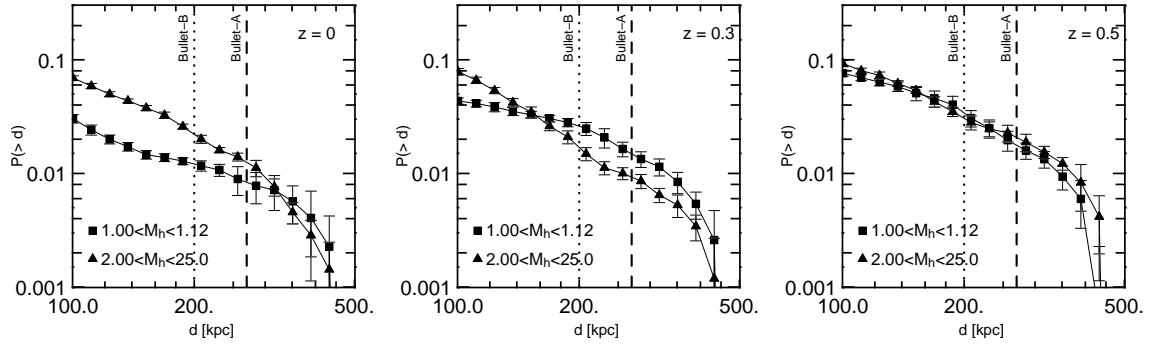


Fig. 2.— Cumulative distribution of 2D displacements between dark matter and gas peaks at redshifts  $z = 0, 0.3$  and  $0.5$  as indicated in the corner of each plot. Triangles represent cluster more massive than  $2.00 \times 10^{14} h^{-1} M_{\odot}$ , squares are clusters with masses between  $1.00 \times 10^{14} h^{-1} M_{\odot}$  and  $1.12 \times 10^{14} h^{-1} M_{\odot}$ .  $M_h$  is given in units of  $1 \times 10^{14} h^{-1} M_{\odot}$ . The upper row shows the 2D displacements in physical units, the lower row normalized by the virial radius of the cluster. The error bars associated to each point are calculated from the variances of 10 different 2D cumulative distributions, computed for different projections of the 3D separations measured in the simulation. The vertical lines in the upper row indicate the displacements for the observed Bullet Cluster (Bullet-A) and the cluster MACS J0025.4-1222 (Bullet-B). The occurrence of a similar or larger displacement is then to be expected in between 1-2 clusters out of 100.

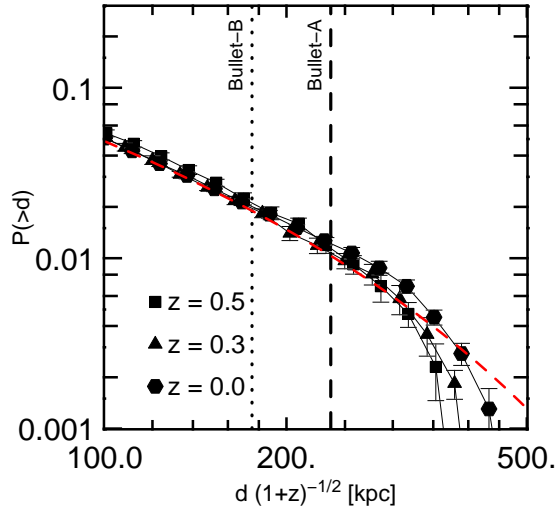


Fig. 3.— Cumulative distribution of 2D physical displacements between dark matter and gas peaks as a function of redshift scaled by  $\sqrt{1+z}$ :  $z = 0$  (hexagons), 0.3 (triangles) and 0.5 (squares). All halos more massive than  $10^{14} h^{-1} M_{\odot}$  were taken into account to make this plot. The vertical lines indicate the measured displacements for the observed Bullet Cluster (Bullet-A) and the cluster MACS J0025.4-1222 (Bullet-B). The red dashed line corresponds to the fitting formula given in Eq.(1).

## 4.2. Scaling with Redshift

In Figure 3 we show the redshift evolution of the cumulative distribution of 2D physical displacements. All clusters more massive than  $10^{14}h^{-1}M_{\odot}$  were taken into account for the construction of these distributions. As can be seen in this Figure, when we consider the rescaled variable  $d/\sqrt{1+z}$ , where  $z$  corresponds to the redshift, the cumulative distributions turn out to be the same for all the redshifts analyzed.

The shape of the cumulative distribution, seems to follow a power law of the displacement until it reaches a critical value, close to the Bullets separations  $\sim 300$  kpc, and then falls off exponentially. A Schechter-like function turns out to be a good fit to the numerical results. In terms of the redshift scaled variable  $d_z = d/\sqrt{1+z}$ :

$$P_{2D} = P_0 \left( \frac{d_z}{d_{\star}} \right)^{\alpha} \exp \left( -\frac{d_z}{d_{\star}} \right), \quad (1)$$

with parameters  $P_0 = 0.04$ ,  $d_{\star} = 200$  kpc and  $\alpha = -1.0$ , fit very well the data shown in Figure 3, in the range  $100 < d_z/\text{kpc} < 500$ .

## 4.3. A toy model to explain the separation dependences

The redshift scaling of the cumulative probability of displacements shown in Fig. 3 calls for an explanation. To this end we resort to previous numerical studies that have followed the dynamics of colliding clusters, in a general context rather than just focusing on reproducing the Bullet Cluster.

There are two important studies that we take as basic references to this end. Tormen et al. (2004) followed the properties of cluster satellites from hydrodynamical cosmological simulations and Poole et al. (2006) studied the impact of mergers on relaxed X-ray clusters, focusing on the dynamical evolution and the emergent transient structures. Both studies were based on numerical simulations which include gas dynamics, but only the latter included cooling and star formation as well. While the work of Tormen et al. (2004) is done in an explicit cosmological setup, in the numerical simulations of Poole et al. (2006) the cosmological context is taken into account in an implicit manner through an adequate selection of the initial conditions. It is relevant to highlight that Poole et al. (2006) find that the results from their simulations compare well with the simple model predictions in Tormen et al. (2004), despite the large differences in the modelling of the baryonic physics.

More specifically, Poole et al. (2006) find that the disruption of the gas substructure is quantitative similar to the results obtained by Tormen et al. (2004) even though the effect

of cooling allows for the formation of denser resilient gas cores. We should also expect that qualitatively, the results presented in this paper would not change much if cooling was included in our simulation. However, a quantitative statement on how the displacements we measured are affected by cooling and star formation processes, would require to run new, high-resolution re-simulations of our clusters. This analysis is well beyond the scope of the present work and will be devoted in further publications on the same topic.

In most of the cases studied by Poole et al. (2006) the central ICM of the merger remnant oscillates with respect to the dark matter distribution. The oscillation of the main ICM remnant can be seen exclusively between the first core interaction and the relaxation of the cluster, a process which lasts between 1Gyr to 3Gyr depending on the mass ratio and the impact parameter of the collision. During this time interval, the core oscillation presents only one large amplitude separation, with the subsequent separation being around half of the first one. A third oscillation shows always an even shorter separation on the order of 50 kpc. One could then simplify the dynamics of the gas-DM separation with the description of damped oscillations, characterized by an initial amplitude, an intrinsic frequency and a damping timescale. Based on the above results, we try now some simple estimations of the scalings of the physical magnitudes in the model.

Let us consider a momentum conserving collision between two gas blobs of mass  $M_g$  and  $m_g$  ( $M_g > m_g$ ), with initial velocities  $V_g = 0$  and  $v_g > 0$ , respectively. Assuming a totally inelastic collision, the velocity of the final blob of mass  $M_g + m_g$  can be expressed as  $V_i = v_g m_g / (M_g + m_g)$ . With the mass ratio definition  $x = M_g / m_g$ , we can rewrite  $V_i = v_g / (x + 1)$ .

N-body simulations of halo mergers have shown that the average velocity of an accreting system into rich cluster type halos is of the same order than the circular velocity,  $V_c$ , of the main cluster, independent of its mass (Tormen 1997; Vitvitska et al. 2002; Poole et al. 2006). We can then approximate  $V_i \sim V_c / (x + 1)$ . Thus, the first initial amplitude of the DM core-core interaction  $A \propto V_c / (x + 1)$ .

The intrinsic frequency of the core-core oscillation can be estimated to be proportional to the apocentric<sup>2</sup> time for the dark matter component of the satellite. The apocentric time encodes the information on the typical dynamical time-scale around the center of the main cluster. Tormen et al. (2004) find that the apocentric times depend only on the mass ratio  $x$ .

---

<sup>2</sup>The apocenter is identified as the first relative maximum in orbital distance measured after the first relative minimum in the satellite orbital distance.

The last element in this description, the intrinsic damping time-scale can be physically related to the same process that unbinds gas and dark matter from the satellite and force their merging. Tormen et al. (2004) find that the decay time to unbind self-bound gas and dark matter particles from the satellite depends mainly on the mass ratio  $x$ .

Summarizing, the separation between gas and DM depends primarily on the circular velocity  $V_c$  of the main cluster and the mass fraction  $x$  of the merging systems. Thus, the larger amplitudes are in principle associated to clusters with larger circular velocities, but depend also on the distribution of mass ratios  $x$ . This might be the reason why we do not see a clear dependence with cluster mass at all redshifts.

Moreover, there is also a redshift dependent scaling relationship between the circular velocity  $V_c$  in physical magnitudes, and the halo mass  $M_h$ . The redshift scaling is such that  $d \propto V_c \propto M_h^{0.35} \sqrt{1+z}$  (Tormen et al. 2004).

In Section 4.2 we considered the displacements of all halos. In this case, the cumulative probability distribution is dominated by the low mass halos simply because of its higher abundance, meaning that we are probing a similar mass range  $\sim 10^{14} h^{-1} M_\odot$  at different redshifts. From the numerical data we find that the distribution of  $d/\sqrt{1+z}$  is redshift independent. This redshift scaling is consistent with the one derived from our toy model,  $d \propto M_h^{0.35} \sqrt{1+z}$ .

#### 4.4. How many Bullets should we expect?

One can now ask the following question: which is the fraction of clusters that will show a separation larger than a given distance? If the volume limited sample is sensitive to halos down to  $10^{14} h^{-1} M_\odot$ , the answer to this question is given by Figure 3: a fraction between 1% and 2% of the clusters presents a separation equal or larger than the Bullet, depending mostly on the redshift, and weakly on the cluster mass, as seen in Figure 2. If we extrapolate these results to clusters with masses larger than in our simulations, we would expect that the fraction of bullet-like displacements will not be very much different (within a factor of  $\sim 2$ ) of the 1-2 % shown here.

### 5. Dependence on Resolution and Power Spectrum Normalization

We will quantify now the dependence of our results on the numerical resolution of the simulations. To this end we compare the cumulative distribution of 2D displacements of DM and gas centers at redshift  $z = 0$  of the simulations MN-1024 and MN-512. The

only difference between the two simulations is the number of particles and the gravitational smoothing. The same seed has been used for the initial conditions.

For this comparison we use the highest mass bin in which we have, in the low resolution simulation, about 4000 DM particles per cluster. This is enough to determine the density peaks with high precision. In the left panel of Figure 4 we show that there is a good agreement between the cumulative probability distribution of the DM-gas displacements in the two simulations with different resolution.

Therefore, we are convinced that our results are not likely to be affected by numerical resolution as long as we have 10.000 or more gas and DM particles available in the clusters under consideration.

Now, we want to use the low resolution simulations to study the dependence of our predictions on the underlying cosmological model. Here we focus again on clusters with more than 4000 DM and gas particles. We compare three models with different normalisation and matter content which are roughly compatible with the WMAP1, 3, and 5 predictions (see Table 1). Yepes et al. (2007) have shown that different  $\sigma_8$  give rise to strong variations in X-ray cluster abundance.

We repeat the analysis presented above using the low resolution simulations MN-512-LS, MN-512 and MN-512-MS. In the right panel of Fig. 4 we show the 2D probability separation distributions for the three lower resolution simulations at redshift  $z = 0$ . We cannot argue for a significant difference in the probability distributions derived from simulations with different  $\sigma_8$ . Although the total number of cluster is different in each simulation, the fraction of clusters showing a give displacement of DM-gas peaks remains almost unchanged.

## 6. Are Bullet Clusters a Challenge to $\Lambda$ CDM?

The recent work by Lee & Komatsu (2010) claims again the difficulty represented by the Bullet Cluster to the  $\Lambda$ CDM cosmology. Their analysis is very similar in spirit to the work of Hayashi & White (2006). Lee & Komatsu (2010) analyze a large volume dark matter only simulation looking for high mass clusters that were not found in the relatively small volume spanned by the Millennium Simulation. The relative velocity of the structure colliding with the main cluster is taken from the study of Mastropietro & Burkert (2008).

The study undertaken by Mastropietro & Burkert (2008) explores the parameter space in a set of idealized cluster collisions. The best mass ratio, impact parameter, and relative velocities of the collision are constrained by assuming that a set of four properties is reason-



ably reproduced: i) the displacements between the X-ray peaks and the mass distribution, ii) the morphology of the bow shock, iii) brightness of the shock and iv) the morphology of the main gas peak. Most of the simulations were performed with a non-radiative treatment of the gas physics. Two different runs out of the total 13 included a crude implementation for cooling. Leaving aside the well known overcooling problem, which affects the main gas peak, the brightness of the shock is strongly modified. Thus the simulated properties of the bow shock are still not well understood and are not yet robustly described by these simulations.

One of the most robust simulated properties is related to the main gas peak. It is well known that a model of cooling without inclusion of energetic feedback does not give a proper description of the gas in the inner part of a cluster (Borgani & Kravtsov 2009). Nevertheless, already the non-radiative description of the gas is a reasonable approximation for the dynamics of the main gas peak (Poole et al. 2006). A complete description of the physics of shocks, should include cooling, star formation and feedback. The fact that the bow shock properties are not robustly described neither in adiabatic nor in radiative runs, weakens the case for its selection as one of the criteria to constrain the success of a certain cosmological model in reproducing the observations. We doubt that the disagreement of the predicted and observed properties of colliding clusters depends only on the parameters of the collisions which are determined by the underlying  $\Lambda$ CDM model.

In other words, simulations of structure formation in the  $\Lambda$ CDM paradigm still do not predict robustly the present very detailed X-ray observations of colliding clusters. Therefore, at present it is difficult (or impossible) to decide whether or not the complete set of observed properties of the cluster 1E0657—56 show a significant anomaly.

In this paper we have taken a much more modest objective, of selecting a single robust property in  $\Lambda$ CDM simulations of clusters, namely the distance between the main dark matter and gas peaks, to work out the significance of the observed anomalies in clusters like 1E0657—56 and MACS J0025.4-1222 . We find that large DM-gas displacements are fairly common in a  $\Lambda$ CDM cosmology. Furthermore our theoretical estimates of the fraction of clusters with large displacements are roughly consistent with the recent observational study of Shan et al. (2010). Therefore, we consider that Bullet Clusters should not be considered as a challenge to  $\Lambda$ CDM.

## 7. Summary and Conclusions

Inspired by the displacement between gaseous and dark component observed in a number of clusters of galaxies, we calculate the distribution of these displacements in a large

cosmological SPH simulation including dark matter and gas.

Theoretically, the mechanism giving rise to these displacements involves a high velocity substructure passing through the center of the parent cluster halo. Assessing the feasibility to accommodate that kind of events in the  $\Lambda$ CDM context, could be used as a test for the validity of the model. Unfortunately, deriving the relative velocity from observations is a non-trivial task, because of statistical and systematical uncertainties, making difficult the comparison to theoretical models.

The separation between the DM and gas components is a much better defined quantity, mostly affected by statistical errors in the measurement process, but not so much by systematic or model-dependent uncertainties.

In this paper we derive, for the first time, the expected physical 2D separation distribution for clusters with a DM mass larger than  $10^{14}h^{-1}M_{\odot}$ . We find that around 1% to 2% of these clusters show DM-gas separations equal or larger than the observed in the Bullet Cluster. Thus, the existence of Bullet Clusters should not be considered as a challenge to the  $\Lambda$ CDM model as it has been recently claimed.

Even though the fractions of expected bullets in our  $\Lambda$ CDM simulation basically coincide with the previous work of Hayashi & White (2006), the comparison between the two results should be taken with a bit of caution. As we mentioned before, the definition of a Bullet cluster in Hayashi & White (2006) is different than in our case. Moreover, the dynamical origin of the large displacements in our clusters seems to be more varied than the scenario of a single dominant substructure passing through the cluster. Nevertheless, the striking coincidence of the predicted bullet fractions between the Millenium N-body simulation and the MareNostrum SPH simulation suggests that indeed it is possible to produce a bullet-like configuration with substructure velocities as low as  $\sim 2400$  km/s.

The approach we use and the results we found are above all a necessary complement to the work of Hayashi & White (2006) and Lee & Komatsu (2010). We give information about the configuration space rather than the velocity space, which can be compared in a more straightforward way to observations as it has been done in the recent work of Shan et al. (2010) on a small sample of 38 clusters, who find an acceptable agreement with our theoretical predictions. The full distribution of these displacements can be considered as new prediction of the  $\Lambda$ CDM model, which could eventually be compared against observations. Upcoming large optical and X-rays surveys can make this feasible in the next years.

### Acknowledgements

The authors acknowledge the work of Claudio Llinares in early stages of the project and Alexander Knebe for his help in setting up his AHF code to be used in our simulations. The MARENOSTRUM UNIVERSE simulation has been done at the Barcelona Supercomputer Center and analyzed at NIC Juelich. GY acknowledges support of MEC (Spain) through research grants FPA2009-08958 and AYA2009-13875-C03-02. We also acknowledge the CONSOLIDER-INGENIO projects MULTIDARK (CSD2009-00064) and SyEC (CSD2007-0050) for supporting our collaboration. We would also like to thank the anonymous referee for her/his valuable comments.

### REFERENCES

- Borgani, S., & Kravtsov, A. 2009, ArXiv e-prints
- Bradač, M., Allen, S. W., Treu, T., Ebeling, H., Massey, R., Morris, R. G., von der Linden, A., & Applegate, D. 2008, ApJ, 687, 959
- Clowe, D., Bradač, M., Gonzalez, A. H., Markevitch, M., Randall, S. W., Jones, C., & Zaritsky, D. 2006, ApJ, 648, L109
- Dopita, M. A., & Sutherland, R. S. 2003, Astrophysics of the diffuse universe, ed. M. A. Dopita & R. S. Sutherland
- Dupke, R. A., Mirabal, N., Bregman, J. N., & Evrard, A. E. 2007, ApJ, 668, 781
- Farrar, G. R., & Rosen, R. A. 2007, Physical Review Letters, 98, 171302
- Gottlöber, S., & Yepes, G. 2007, ApJ, 664, 117
- Hayashi, E., & White, S. D. M. 2006, MNRAS, 370, L38
- Heymans, C., Gray, M. E., Peng, C. Y., van Waerbeke, L., Bell, E. F., Wolf, C., Bacon, D., Balogh, & et al. 2008, MNRAS, 385, 1431
- Jee, M. J., Ford, H. C., Illingworth, G. D., White, R. L., Broadhurst, T. J., Coe, D. A., Meurer, G. R., van der Wel, A., Benítez, N., Blakeslee, J. P., Bouwens, R. J., Bradley, L. D., Demarco, R., Homeier, N. L., Martel, A. R., & Mei, S. 2007, ApJ, 661, 728
- Jee, M. J., White, R. L., Benítez, N., Ford, H. C., Blakeslee, J. P., Rosati, P., Demarco, R., & Illingworth, G. D. 2005a, ApJ, 618, 46

- Jee, M. J., White, R. L., Ford, H. C., Blakeslee, J. P., Illingworth, G. D., Coe, D. A., & Tran, K.-V. H. 2005b, *ApJ*, 634, 813
- Klypin, A., Gottlöber, S., Kravtsov, A. V., & Khokhlov, A. M. 1999, *ApJ*, 516, 530
- Knollmann, S. R., & Knebe, A. 2009, *ApJS*, 182, 608
- Lee, J., & Komatsu, E. 2010, ArXiv e-prints
- Mahdavi, A., Hoekstra, H., Babul, A., Balam, D. D., & Capak, P. L. 2007, *ApJ*, 668, 806
- Mastropietro, C., & Burkert, A. 2008, *MNRAS*, 389, 967
- Nusser, A. 2008, *MNRAS*, 384, 343
- Poole, G. B., Fardal, M. A., Babul, A., McCarthy, I. G., Quinn, T., & Wadsley, J. 2006, *MNRAS*, 373, 881
- Qin, B., Shan, H., & Tilquin, A. 2008, *ApJ*, 679, L81
- Shan, H., Quin, B., Fort, B., Tao, C., Wu, X.-P., & Zhao, H. 2010, *MNRAS* accepted
- Spergel, D. N., Bean, R., Doré, O., Nolta, M. R., Bennett, C. L., Dunkley, J., Hinshaw, G., Jarosik, N., Komatsu, E., Page, L., Peiris, H. V., Verde, L., Halpern, M., Hill, R. S., Kogut, A., Limon, M., Meyer, S. S., Odegard, N., Tucker, G. S., Weiland, J. L., Wollack, E., & Wright, E. L. 2007, *ApJS*, 170, 377
- Springel, V. 2005, *MNRAS*, 364, 1105
- Springel, V., & Farrar, G. R. 2007, *MNRAS*, 380, 911
- Springel, V., White, S. D. M., Jenkins, A., Frenk, C. S., Yoshida, N., Gao, L., Navarro, J., Thacker, R., Croton, D., Helly, J., Peacock, J. A., Cole, S., Thomas, P., Couchman, H., Evrard, A., Colberg, J., & Pearce, F. 2005, *Nature*, 435, 629
- Tormen, G. 1997, *MNRAS*, 290, 411
- Tormen, G., Moscardini, L., & Yoshida, N. 2004, *MNRAS*, 350, 1397
- Vitvitska, M., Klypin, A. A., Kravtsov, A. V., Wechsler, R. H., Primack, J. R., & Bullock, J. S. 2002, *ApJ*, 581, 799
- Yepes, G., Sevilla, R., Gottlöber, S., & Silk, J. 2007, *ApJ*, 666, L61

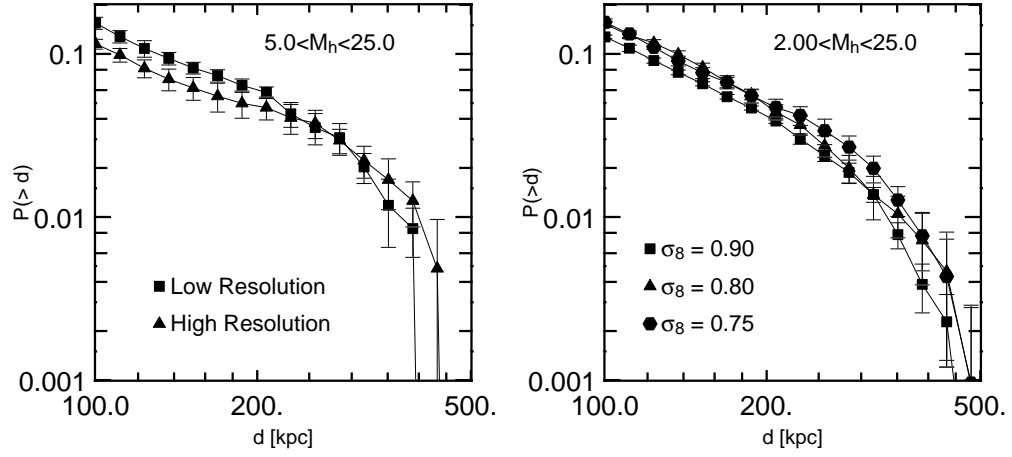


Fig. 4.— Left panel: Cumulative distributions of 2D displacements for simulations with different mass resolutions. Right panel: Cumulative distributions of 2D displacements for simulations with different power spectrum normalizations  $\sigma_8$ .  $M_h$  is given in  $10^{14}h^{-1}M_\odot$ .